2018 UKACC 12th International Conference on Control (CONTROL)
Sheffield, UK, 5-7 Sept 2018

Cooperative Control of Innovative Tri-rotor Drones Using Robust Feedback Linearization

Junyan Hu
School of Electrical and Electronic Engineering
The University of Manchester
Manchester, UK
Junyan.Hu@manchester.ac.uk

Alexander Lanzon
School of Electrical and Electronic Engineering
The University of Manchester
Manchester, UK
Alexander.Lanzon@manchester.ac.uk

***Abstract*—This paper presents a novel distributed formation control architecture for innovative tri-rotor drones. The three rotors of this novel aerial robotic platform can be tilted independently to obtain full force and torque vectoring authority, such that the tri-rotor drone is able to overcome the limitations of a classic quadrotor UAV that can not change its attitude while hovering at a stationary position. In the flight control systems design, a robust feedback linearization controller is first developed to handle the highly coupled and nonlinear dynamics and a distributed adaptive formation control tracking protocol is then designed to control a swarm of tri-rotor UAVs. The 3D position and 3D attitude of each vehicle can be controlled independently to follow a desired formation. The effectiveness of the proposed control strategy is shown via a realistic virtual reality simulation environment that the networked tri-rotor drones are robust to aerodynamic disturbances and model uncertainties.**

***Index Terms*—Aerial robotics, adaptive control, multi-agent systems, unmanned Aerial Vehicle**

I. Introduction

In recent years, distributed cooperative control of multi-agent systems have received significant attention from both the practical engineering and academic communities due to their broad prospect in applications, such as unmanned aerial vehicles formation, multi-robot cooperation, distributed sensor networks, etc. The research field includes consensus control [1], rendezvous control, containment control, and formation control. Formation control of multi-agent systems is hence a key active area of research, which has experienced a rapid growth in the research efforts from the international robotics community.

Recently, many consensus-based control methods have been applied to solve formation control problems. Motion trajectory tracing and formation control of first-order and second-order multi-robot systems are presented in [2] and [3], respectively. [4] discusses the formation stability problems for general high-order swarm systems, and the result is extended to deal with formation tracking for multiple high-order autonomous agents by using a two-level consensus approach in [5]. Formation control of quadrotor swarm systems based on consensus strategies is achieved in [6] and [7], while distributed cooperative control of innovative aerial robotic platforms is still a vigorously active research topic with much progress still needed.

This work was supported by the Engineering and Physical Sciences Research Council (EPSRC) [grant number EP/R008876/1]. All research data supporting this publication are directly available within this publication.

Fig. 1. The hardware of the designed tri-rotor UAV

Aiming at more efficient configurations in terms of size, autonomy, flight range, and payload capacity, some innovative vehicle platforms are developed by researchers in recent years [8]. The proposed tri-rotor UAV (as shown in Fig. 1) has three rotors arranged in an equilateral triangular configuation and each rotor is attached to a servo motor that can independently change the rotating direction of the propeller. Thus, complete 3D thrust and 3D torque vectoring authority is achieved.. This configuration guarantees the UAV a high level of flexibility and maneuverability for attitude control and position movement, such characteristics allow the UAV to fly easier in narrow space and create possibility to avoid obstacles. Compared to the quadrotor, this innovative configuration also requires less hover power and hence provides longer flight time, which makes it ideal for deployment in various missions.

The dynamics of the proposed tri-rotor UAVs are highly coupled and nonlinear, which presents a significant challenge to control system design. In contrast to a quadrotor UAV, which has zero angular momentum in hover, a tri-rotor UAV has persistent angular moment, and hence also gyroscopic dynamics due to the asymmetric configuration of the system which poses significant control systems complexities.

Motivated by the challenges stated above, the combination of formation control and the proposed innovative tri-rotor drone is developed and investigated in this paper. Robust feedback linearization is used to handle the tri-rotor drone's

highly coupled and nonlinear dynamics. It has been successfully demonstrated [9] to provide significant robustness to both model uncertainty and external dynamics. A cooperative adaptive state feedback formation protocol is also applied to the networked tri-rotor UAV swarm, which is based on neighboring information without using global information of the communication graph. It is shown that the proposed strategy provides a straightforward way to construct fully distributed controllers that ensure stabilization and synchronization of the swarm.

Throughout this paper, let $I_n \in \mathbb{R}^{n\times n}$ denote the identity matrix of demension n and $\mathbf{1}_N \in \mathbb{R}^n$ be the vector with all entries equal to one. $\mathrm{diag}\{a_i\}$ represents a diagonal matrix with diagonal entries a_i. The Kronecker product is denoted by $\otimes$.

II. Preliminaries on Graph Theory

Consider a weighted and directed graph $\mathcal{G} = (\mathcal{V}, \mathcal{E}, \mathcal{A})$ with a nonempty set of N nodes $\mathcal{V} = \{1, 2, \ldots, N\}$, a set of edges $\mathcal{E} \subset \mathcal{V} \times \mathcal{V}$, and associated adjacency matrix $\mathcal{A} = [a_{ij}] \in \mathbb{R}^{N\times N}$. An edge rooted at node i and ended at node j is denoted by (i, j), which means information can flow from node i to node j. a_{ij} is the weight of edge (i, j) and $a_{ij} > 0$ if $(i, j) \in \mathcal{E}$. Assume that there are no repeated edges and no self loops. Node j is called a neighbour of node i if $(i, j) \in \mathcal{E}$. A directed graph has or contains a directed spanning tree if there exists a node, called the root, such that there exists a directed path from this node to every other nodes.

Lemma 1 ([10]): If $\mathcal{G}$ contains a spanning tree, then zero is a simple eigenvalue of L with associated right eigenvector $\mathbf{1}_N$, and all the other $N-1$ eigenvalues have nonnegative real parts.

Lemma 2 ([11]): Consider a nonsingular M-matrix L. There exists a diagonal matrix G such that $G = \mathrm{diag}\{g_1, \ldots, g_N\} > 0$ and $GL + L^T G > 0$

Lemma 3 ([12]): If a and b are nonnegative real numbers and p and q are positive real numbers such that $\frac{1}{p} + \frac{1}{q} = 1$, then $ab \le \frac{a^p}{p} + \frac{b^q}{q}$, equality holds if and only $a^p = b^q$.

The following assumption of graph topology holds throughout this paper.

Assumption 1: The directed graph $\mathcal{G}$ contains a spanning tree and the root node i can obtain information from the leader node.

III. Mathematical Modeling

The configuration of the tri-rotor UAV was first proposed in our earlier work [13], [14]. In order to develop the dynamic model of the proposed tri-rotor UAV, the following right hand coordinate systems shown in Fig. 2 are considered: (X_e, Y_e, Z_e) represents the earth coordinate system, which is assumed to be inertial (i.e. fixed). (X_b, Y_b, Z_b) denotes the body coordinate system, where the origin O_b is fixed to the center of mass of the vehicle. This coordinate system moves with the vehicle. (X_{li}, Y_{li}, Z_{li}) with $i \in \{1, 2, 3\}$ is the local coordinate system of each propeller-motor assembly.

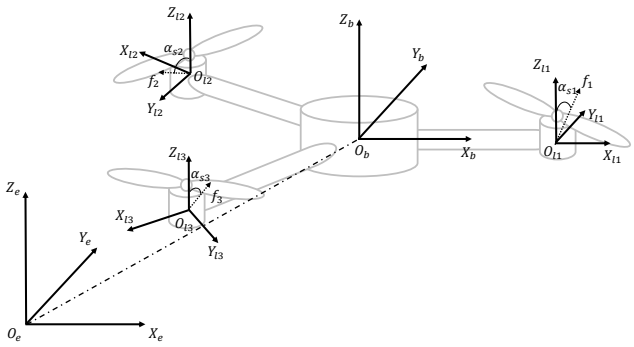

Fig. 2. Coordinate systems of the tri-rotor UAV

TABLE I
Notation of the tri-rotor UAV model

Symbol	Defination
ω_{mi}	Rotational speed of the ith DC motor
α_{si}	Tilting angle of the ith servo motor
k_f	Thrust-to-speed constant of the propeller
k_d	Torque-to-speed constant of the propeller
g	Gravitational acceleration
m	Total mass of the UAV
I_v^b	Inertia matrix of the UAV
κ_v^b	The transitional velocity of the UAV
u_b, v_b, w_b	The Cartesian coordinates of the UAV transitional velocity
ω_v^b	Angular velocity of the UAV
p, q, r	The Cartesian coordinates of the UAV angular velocity
η_v	Attitude vector of the UAV related to the earth frame
λ_v^e	Position vector of the UAV (earth frame)
ϕ	Roll angle of the UAV related to the earth frame
θ	Pitch angle of the UAV related to the earth frame
ψ	Yaw angle of the UAV related to the earth frame
x_v	The x coordinate position of the UAV in the earth frame
y_v	The y coordinate position of the UAV in the earth frame
z_v	The z coordinate position of the UAV in the earth frame
R_b^e	The rotational matrix from frame b to frame e

It is assumed that the UAV has fast servo dynamics, which results in instantaneous change of tilting angles.

The dynamic model of the tri-rotor can be described in a compact form as

$$\dot{\kappa}_v^b = g\Theta - S(\omega_v^b)\kappa_v^b + \frac{k_f}{m} H_f \rho, \tag{1}$$

$$\dot{\omega}_v^b = -(I_v^b)^{-1} S(\omega_v^b) I_v^b \omega_v^b + (I_v^b)^{-1}(k_f H_t - k_d H_f)\rho, \tag{2}$$

$$\dot{\eta}_v = \Psi \omega_v^b, \tag{3}$$

$$\dot{\lambda}_v^e = R_b^e \kappa_v^b, \tag{4}$$

where all terms used in the model of the UAV are defined in Table 1 and

$$\kappa_v^b = \begin{bmatrix} u_b \\ v_b \\ w_b \end{bmatrix},\ \omega_v^b = \begin{bmatrix} p \\ q \\ r \end{bmatrix},\ \eta_v = \begin{bmatrix} \phi \\ \theta \\ \psi \end{bmatrix} \text{ and } \lambda_v^e = \begin{bmatrix} x_v \\ y_v \\ z_v \end{bmatrix}.$$

The remaining matrices are defined as:

$$H_f = \begin{bmatrix} 0 & -\frac{\sqrt{3}}{2} & \frac{\sqrt{3}}{2} & 0 & 0 & 0 \\ 1 & -\frac{1}{2} & -\frac{1}{2} & 0 & 0 & 0 \\ 0 & 0 & 0 & 1 & 1 & 1 \end{bmatrix},\quad \Theta = \begin{bmatrix} \sin(\theta) \\ -\sin(\phi)\cos(\theta) \\ -\cos(\phi)\cos(\theta) \end{bmatrix},$$

and

$$H_t = l \begin{bmatrix} 0 & 0 & 0 & 0 & \frac{\sqrt{3}}{2} & -\frac{\sqrt{3}}{2} \\ 0 & 0 & 0 & -1 & \frac{1}{2} & \frac{1}{2} \\ 1 & 1 & 1 & 0 & 0 & 0 \end{bmatrix}.$$

We can choose the state vector as

$$\begin{aligned} x &= [x_1 \;\; x_2 \;\; x_3 \;\; x_4 \;\; x_5 \;\; x_6 \;\; x_7 \;\; x_8 \;\; x_9 \;\; x_{10} \;\; x_{11} \;\; x_{12}]^T \\ &= [u_b \;\; v_b \;\; w_b \;\; p \;\; q \;\; r \;\; \phi \;\; \theta \;\; \psi \;\; x_v \;\; y_v \;\; z_v]^T, \end{aligned}$$

and the input and output vectors as

$$u = \rho = \begin{bmatrix} u_1 \\ u_2 \\ u_3 \\ u_4 \\ u_5 \\ u_6 \end{bmatrix} = \begin{bmatrix} \omega_{m1}^2 \sin(\alpha_{s1}) \\ \omega_{m2}^2 \sin(\alpha_{s2}) \\ \omega_{m3}^2 \sin(\alpha_{s3}) \\ \omega_{m1}^2 \cos(\alpha_{s1}) \\ \omega_{m2}^2 \cos(\alpha_{s2}) \\ \omega_{m3}^2 \cos(\alpha_{s3}) \end{bmatrix}, \; y = \begin{bmatrix} \phi \\ \theta \\ \psi \\ x_v \\ y_v \\ z_v \end{bmatrix} = \begin{bmatrix} x_7 \\ x_8 \\ x_9 \\ x_{10} \\ x_{11} \\ x_{12} \end{bmatrix}.$$

IV. Control System Design

The objective of this section is to design a robust distributed formation control protocol for swarms of the proposed tri-rotor UAV. Since the dynamical model of a single tri-rotor UAV is highly coupled and nonlinear, a robust feedback linearization technique is first applied to each tri-rotor to obtain simpler closed-loop dynamics. Then the swarm of identical tri-rotor UAVs is controlled through a distributed adaptive formation control protocol which solves the formation tracking problem for tri-rotor robotic swarms as shown in Fig. 3.

A. Robust Feedback Linearization

The nonlinear dynamics of the tri-rotor UAV can be described by

$$\dot{x} = F(x) + G(x)\,u = F(x) + \sum_{i=1}^{m} G_i(x)\,u_i, \tag{5}$$

$$y = [H_1(x), \ldots, H_m(x)]^T, \tag{6}$$

where $x(t) \in \mathbb{R}^n$ denotes the state vector, $u(t) \in \mathbb{R}^m$ is the control input, $y(t) \in \mathbb{R}^m$ is the output vector, and $F(x)$, $G_1(x), \ldots, G_m(x)$, $H_1(x), \ldots, H_m(x)$ are smooth vector fields defined on an open subset of $\mathbb{R}^n$.

It can be seen that this system satisfies the well-known conditions for feedback linearization [15]: The relative degree of H_i is equal to r_i for $i \in \{1, \ldots, m\}$ such that $r_1 + \cdots + r_m = n$, and the decoupling matrix

$$M(x) = \begin{bmatrix} L_{G_1} L_f^{r_1 - 1} H_1(x) & \ldots & L_{G_m} L_f^{r_1 - 1} H_1(x) \\ \vdots & \ddots & \vdots \\ L_{G_1} L_f^{r_m - 1} H_m(x) & \ldots & L_{G_m} L_f^{r_m - 1} H_m(x) \end{bmatrix} \tag{7}$$

is invertible, where $L_{(.)}(.)$ denotes the Lie derivative operator [15]. It is then possible to find a feedback linearizing control law of the form

$$u(x, w) = \alpha_c(x) + \beta_c(x)\,w, \tag{8}$$

where $w(t)$ is a new control input, and $\alpha_c(x) = -M^{-1}(x) \left[L_f^{r_1} H_1(x) \;\; \ldots \;\; L_f^{r_m} H_m(x) \right]^T$, $\beta_c(x) = M^{-1}(x)$, such that on application of the control law in (8), the nonlinear state-equation (5) reduces into the linear state-equation

$$\dot{x}_c = A_c x_c + B_c w, \tag{9}$$

where A_c and B_c are matrices of the Brunovsky canonical form [15], and a change of coordinates $x_c = \phi_c(x)$ with $\phi_c^T(x) = \left[\phi_{c1}^T(x) \;\; \ldots \;\; \phi_{cm}^T(x) \right]$ and $\phi_{ci}^T(x) = [H_i(x) \;\; L_f H_i(x) \;\; \ldots \;\; L_f^{r_i - 1} H_i(x)]$.

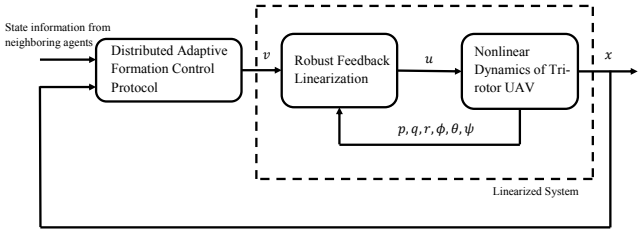

Fig. 3. Control system scheme: Distributed optimal formation control law and robust feedback linearization combining linear and nonlinear parts

The robust feedback linearization technique [16], on the other hand, exactly transforms the nonlinear state-equation into a linear state-equation that is equal to the Jacobi linear approximation of the original nonlinear state-equation around the origin. The nonlinear state-equation (5) is geometrically transformed into the linear state-equation of any operating point, not only in a small neighborhood of the origin point.

The robust feedback linearization control law is

$$u(x, v) = \alpha(x) + \beta(x)\,v, \tag{10}$$

where $v(t)$ is a new control input, and

$$\alpha(x) = \alpha_c(x) + \beta_c(x)\,LU^{-1}\phi_c(x), \tag{11}$$

$$\beta(x) = \beta_c(x)\,R^{-1}, \tag{12}$$

$$\phi_r(x) = U^{-1}\phi_c(x), \tag{13}$$

$$L = -M(0)\,\partial_x \alpha_c(0), \tag{14}$$

$$R = M^{-1}(0), \tag{15}$$

$$U = \partial_x \phi_c(0). \tag{16}$$

After calculating the classic Brunowski form linearizing input (8) and applying the formulas for the robust feedback linearization (10)-(16), the system can then be robust feedback linearized into

$$\dot{x}_r = A_r x_r + B_r v, \tag{17}$$

where $A_r = \partial_x F(0)$ and $B_r = G(0)$.

Furthermore, ϕ_c and ϕ_r are given by

$$\phi_c = [x_7 \; x_8 \; x_9 \; x_{10} \; x_{11} \; x_{12} \; \dot{x}_7 \; \dot{x}_8 \; \dot{x}_9 \; \dot{x}_{10} \; \dot{x}_{11} \; \dot{x}_{12}]^T,$$

$$\phi_r = [\dot{x}_{10} \; \dot{x}_{11} \; \dot{x}_{12} \; \dot{x}_7 \; \dot{x}_8 \; \dot{x}_9 \; x_7 \; x_8 \; x_9 \; x_{10} \; x_{11} \; x_{12}]^T.$$

From [16] we know the change of coordinates after robust feedback linearization is $x_r = \phi_r(x)$.

B. Distributed Adaptive Formation Protocol Design

Consider a group of N tri-rotor UAVs. Suppose that each tri-rotor UAV has the identical linearized dynamics described by

$$\dot{x}_{ri} = A_r x_{ri} + B_r v_i. \tag{18}$$

It can be easily verified that (A_r, B_r) is stabilizable.

The dynamics of the leader node, labeled 0, is given by

$$\dot{x}_0 = A_r x_0, \tag{19}$$

where $x_0 \in \mathbb{R}^n$ is the state. It can be considered as a command generator, which generates the desired target trajectory. The leader can be observed from a subset of UAVs in a graph. If agent i observes the leader, an edge $(0, i)$ is said to exist with weighting gain $a_{i0} > 0$ as a pinned node.

Then the Laplacian matrix L related to $\mathcal{G}$ can be partitioned as $L = \begin{bmatrix} 0 & 0_{1\times N} \\ L_2 & L_1 \end{bmatrix}$.

The desired formation is specified by the vector $h = \left[h_1^T, h_2^T, \ldots, h_N^T\right]^T$ with $h_i \in \mathbb{R}^n$ being a preset vector known by the corresponding i^{th} agent. The tri-rotor swarm is said to achieve formation tracking if for any given bounded initial states

$$\lim_{t\to\infty} (x_{ri}(t) - h_i(t) - x_0(t)) = 0 \ \forall i \in \{1, \ldots, N\}. \tag{20}$$

Construct the following fully distributed adaptive formation control protocol

$$\begin{aligned} v_i &= F x_{ri} + (c_i + \rho_i) K \xi_i + \gamma_i, \\ \dot{c}_i &= \xi_i^T \Gamma \xi_i \quad \forall i \in \{1, \ldots, N\}, \end{aligned} \tag{21}$$

where $\xi_i = \sum_{j=0}^{N} a_{ij}(t)[(x_{ri} - h_i) - (x_{rj} - h_j)]$, $c_i(t)$ denotes the time varying coupling weight associated with the ith agent with $c_i(0) \geq 0$, $F \in \mathbb{R}^{m\times n}$, $K \in \mathbb{R}^{p\times n}$ and $\Gamma \in \mathbb{R}^{n\times n}$ are the feedback gain matrices, and ρ_i and γ_i are smooth functions to be determined.

Since the matrix B_r given in (18) is of full rank, there always exists a nonsingular matrix $[\tilde{B}^T, \bar{B}^T]^T$ with $\tilde{B} \in \mathbb{R}^{m\times n}$ and $\bar{B} \in \mathbb{R}^{(n-m)\times n}$ such that $\tilde{B}B_r = I_m$ and $\bar{B}B_r = 0$.

Theorem 1: Suppose that Assumption 1 holds. If the following formation feasibility condition is satisfied

$$\bar{B}[(A_r + B_r F)h_i - \dot{h}_i] = 0 \ \forall i \in \{1, \ldots, N\}, \tag{22}$$

the formation specified by $h_i \in \mathbb{R}^n \ \forall i \in \{1, \ldots, N\}$ can be achieved under the distributed adaptive control protocol (21) with $K = -R^{-1}B_r^T P$, $\Gamma = PB_rR^{-1}B_r^T P$, $\gamma_i = \tilde{B}[\dot{h}_i - (A_r + B_r F)h_i]$ and $\rho_i = \xi_i^T P \xi_i$, where $P > 0$ is a solution to the following Riccati equation:

$$(A_r + B_r F)^T P + P(A_r + B_r F) + Q - PB_rR^{-1}B_r^T P = 0 \tag{23}$$

with $Q > 0$ and $R > 0$.

Proof: Let the global consensus error $\xi = [\xi_1^T, \ldots, \xi_N^T]^T$. Define $z_i = x_{ri} - h_i \ \forall i \in \{1, \ldots, N\}$ and $z = [z_1^T, \ldots, z_N^T]^T$. Therefore, the global error vector can be written in a compact form as

$$\begin{aligned} \xi =& (L_1 \otimes I_n)z + (L_2 \otimes I_n)x_0 \\ =& (L_1 \otimes I_n)(z - \mathbf{1} \otimes x_0). \end{aligned} \tag{24}$$

Substituting (21) into (18), the following dynamics of ξ and c_i can be obtained

$$\begin{aligned} \dot{\xi} =& [I_N \otimes (A_r + B_r F) + L_1(C + \rho) \otimes B_r K]\xi \\ &+ [L_1 \otimes (A_r + B_r F)]h - (L_1 \otimes I_n)\dot{h} + (L_1 \otimes B_r)\gamma, \\ \dot{c}_i =& \xi_i^T \Gamma \xi_i \quad \forall i \in \{1, \ldots, N\}, \end{aligned} \tag{25}$$

where $C = \mathrm{diag}\{c_1, \ldots, c_N\}$, $\rho = \mathrm{diag}\{\rho_1, \ldots, \rho_N\}$, and $\gamma = \left[\gamma_1^T, \gamma_2^T, \ldots, \gamma_N^T\right]^T$.

Consider the following Lyapunov function candidate

$$V_1 = \sum_{i=1}^{N} \frac{1}{2} g_i (2c_i + \rho_i)\rho_i + \frac{1}{2}\sum_{i=1}^{N} g_i (c_i - \alpha)^2 \tag{26}$$

where $G = \mathrm{diag}\{g_1, \ldots, g_N\}$ is a positive definite matrix such that $GL_1 + {L_1}^T G > 0$, and α is a positive constant to be determined later. According to Lemma 1 and the fact that L_1 is a nonsingular M-matrix, the existence of such a positive definite matrix G can be guaranteed from Lemma 2. Because $c_i(0) > 0$, it follows from $\dot{c}_i(t) \geq 0$ that $c_i(t) > 0$ for any $t > 0$. Then, it is easy to conclude that V_1 is positive definite.

Thus, the time derivative of V_1 along the trajectory of (25) is obtained as

$$\begin{aligned} \dot{V}_1 &= \sum_{i=1}^{N} [g_i(c_i + \rho_i)\dot{\rho}_i + g_i \rho_i \dot{c}_i] + \sum_{i=1}^{N} g_i (c_i - \alpha)\dot{c}_i \\ &= \sum_{i=1}^{N} 2g_i(c_i + \rho_i)\xi_i^T P \dot{\xi}_i + \sum_{i=1}^{N} g_i(\rho_i + c_i - \alpha)\dot{c}_i \end{aligned} \tag{27}$$

Note that

$$\sum_{i=1}^{N} g_i(\rho_i + c_i - \alpha)\dot{c}_i = \xi^T[(C + \rho - \alpha I)G \otimes \Gamma]\xi, \tag{28}$$

and

$$\begin{aligned} &\sum_{i=1}^{N} 2g_i(c_i + \rho_i)\xi_i^T P \dot{\xi}_i = 2\xi^T[(C + \rho)G \otimes P]\dot{\xi} \\ =& \xi^T[(C + \rho)G \otimes [P(A_r + B_r F) + (A_r + B_r F)^T P] \\ &- (C + \rho)(GL_1 + L_1^T G)(C + \rho) \otimes \Gamma]\xi \\ &+ 2\xi^T[(C + \rho)GL_1 \otimes P(A_r + B_r F)]h \\ &- 2\xi^T[(C + \rho)GL_1 \otimes P]\dot{h} \\ &+ 2\xi^T[(C + \rho)GL_1 \otimes PB_r]\gamma \\ \leq& \xi^T[(C + \rho)G \otimes [P(A_r + B_r F) + (A_r + B_r F)^T P] \\ &- \lambda_0^{min}(C + \rho)^2 \otimes \Gamma]\xi \\ &+ 2\xi^T[(C + \rho)GL_1 \otimes P(A_r + B_r F)]h \\ &- 2\xi^T[(C + \rho)GL_1 \otimes P]\dot{h} \\ &+ 2\xi^T[(C + \rho)GL_1 \otimes PB_r]\gamma \end{aligned} \tag{29}$$

where λ_0^{min} represents the minimum of the smallest positive eigenvalue of $GL_1 + L_1^T G$.

If condition (22) holds, then for all $i \in \{1, \ldots, N\}$

$$\bar{B}(A_r + B_r F)h_i - \bar{B}\dot{h}_i + \bar{B}B_r\gamma_i = 0. \tag{30}$$

By letting $\gamma_i = \tilde{B}\dot{h}_i - \tilde{B}(A_r + B_rF)h_i$, it follows that

$$\tilde{B}(A_r + B_rF)h_i - \tilde{B}\dot{h}_i + \tilde{B}B_r\gamma_i = 0. \tag{31}$$

From (30) and (31) and the fact that $\left[\tilde{B}^T, \bar{B}^T\right]^T$ is nonsingular, one gets

$$(A_r + B_rF)h_i - \dot{h}_i + B_r\gamma_i = 0, \tag{32}$$

which means that

$$\left[I_N \otimes (A_r + B_rF)\right] h - (I_N \otimes I_N)\dot{h} + (I_N \otimes B_r)\,\gamma = 0. \tag{33}$$

Pre-multiplying the both sides of (33) by $(C + \rho)GL_1 \otimes P$ yields

$$\begin{aligned}\left[(C + \rho)GL_1 \otimes P(A_r + B_rF)\right]h - \left[(C + \rho)GL_1 \otimes P\right]\dot{h} \\ + \left[(C + \rho)GL_1 \otimes PB_r\right]\gamma = 0.\end{aligned} \tag{34}$$

Therefore, we obtain

$$\begin{aligned}\dot{V}_1 \leq & \xi^T\left[(C + \rho)G \otimes [P(A_r + B_rF) + (A_r + B_rF)^T P \right. \\ & \left. + \Gamma] - (\lambda_0^{min}(C + \rho)^2 + \alpha G) \otimes \Gamma\right]\xi.\end{aligned} \tag{35}$$

From Lemma 3, we have

$$\begin{aligned}& - \xi^T(\lambda_0^{min}(C + \rho)^2 + \alpha G) \otimes \Gamma]\xi \\ \leq & - 2\xi^T[\sqrt{\lambda_0^{min}\alpha G}(C + \rho) \otimes \Gamma]\xi.\end{aligned} \tag{36}$$

Selecting $\alpha \geq \frac{\max_{i\in\{1,\ldots,N\}} g_i}{\lambda_0^{min}}$ and substituting (36) into (35) yields

$$\dot{V}_1 \leq \xi^T\left[(C+\rho)G\otimes[P(A_r+B_rF)+(A_r + B_rF)^T P - \Gamma]\right]\xi. \tag{37}$$

Define $\zeta = (\sqrt{(C + \rho)G} \otimes I)\xi$. Therefore, it follows from (37) that

$$\begin{aligned}\dot{V}_1 \leq & \zeta^T\left[I_N \otimes [P(A_r + B_rF) + (A_r + B_rF)^T P \right. \\ & \left. - PB_rR^{-1}B_r{}^T P]\right]\zeta \\ \leq & 0\end{aligned} \tag{38}$$

where the last inequality comes immediately from the Riccati equation (23). Since $V_1(t) \geq 0$ and $\dot{V}_1(t) \leq 0$, $V_1(t)$ is bounded. $\dot{V}_1 \equiv 0$ implies $\zeta \equiv 0$, which in turn implies that $\xi \equiv 0$. By using LaSalle's invariance principle, we have the formation tracking error ξ asymptotically converges to zero. Therefore, the distributed formation tracking of tri-rotor UAVs is achieved. ■

Remark 1: It should be noted that the formation control problem reduces to a consensus problem when $h_i = 0$ $\forall i \in \{1, \ldots, N\}$, such that the protocol shown in [17] can be viewed as a special case of the result in the current paper.

Remark 2: The proposed distributed adaptive formation tracking protocol in this paper is different from that in [18], where it is necessary to calculate the minimum positive eigenvalue of the Laplacian matrix of the communication topology. Our distributed cooperative controller allows each drone only to access the information from its neighbors such that the proposed controller is fully distributed regardless of global information.

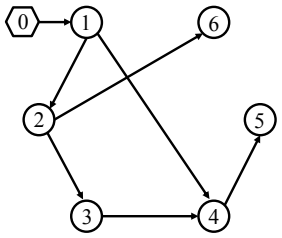

Fig. 4. Directed interaction topology $\mathcal{G}$

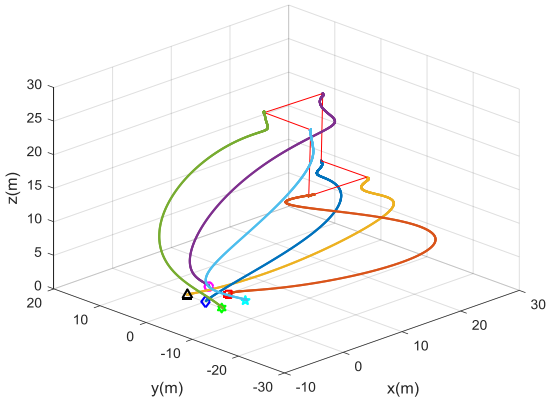

Fig. 5. 3D trajectories of the tri-rotor swarm

V. Simulation Results

The numerical simulation is carried out in this section in order to validate the theoretical results.

The simulation environment has been designed and implemented in Simscape Multibody™ and Simulink® for more realistic results as this provides a 3D graphical display of physical devices. Simscape Multibody™ is used to develop the dynamic model of the tri-rotor UAV based on physical components and the designed control system is implemented in Simulink®. The actuator delay and aerodynamic parameters are measured via experimentation.

The directed interaction topology among the six vehicles is shown in Fig. 4, where the leader agent 0 provides the formation reference signal. Recall that $h_i \in \mathbb{R}^n$ is the formation offset vector with respect to the formation reference $x_0 \in \mathbb{R}^n$. The 3D attitude and 3D position of each UAV are chosen independently. The control parameters K and Γ can be chosen by the procedure in Theorem 1. Smooth functions ρ_i and γ_i can then be determined subsequently. The proposed control strategy is valid regardless of the leader is static or time-varying.

On using robust control law (10) with distributed adaptive formation control protocol (21), the trajectory of each tri-rotor UAV is given by Fig. 5. The attitude tracking performance with respect to roll, pitch and yaw angles and the position tracking of hovering are shown in Fig. 6. The 3D visualization of distributed formation of the tri-rotor UAV swarm are illustrated in Fig. 7. From all these figures, it can be seen that the tri-rotor swarm forms an expected formation after 15s. It is concluded

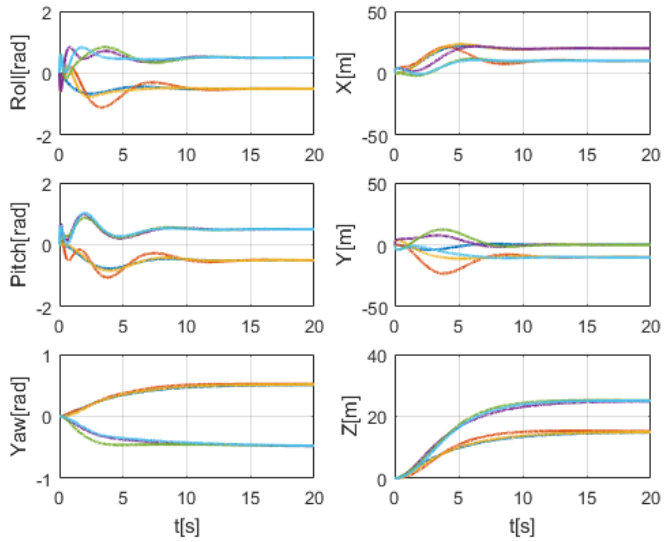

Fig. 6. Attitude and position response of the tri-rotor swarm.

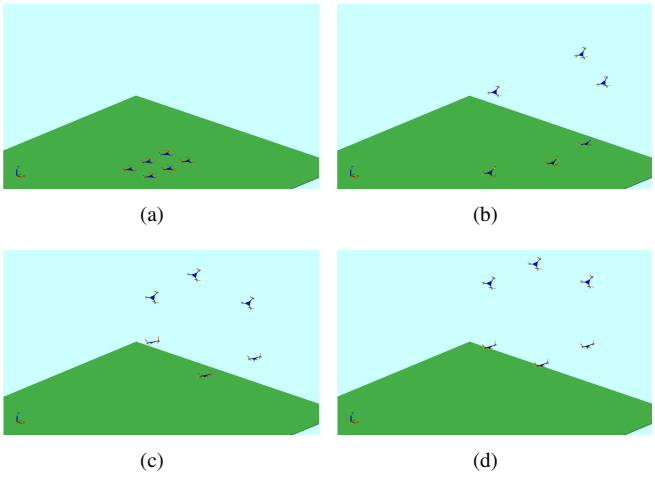

Fig. 7. 3D shots of the tri-rotor swarm system. (a) $t = 0$ s. (b) $t = 5$ s. (c) $t = 10$ s. (d) $t = 20$ s.

that the desired formation and attitude tracking of the UAV swarm is achieved independently, and the designed control system preserves good robustness properties when subjected to simulated aerodynamic disturbances and model uncertainties.

VI. Conclusion

In this paper, we have solved a formation tracking problem of a networked tri-rotor UAV swarm by using a distributed adaptive formation control protocol. It has been shown that the proposed tri-rotor UAV swarm is able to track a desired formation whilst independently tracking different attitudes, which lays the foundation for some more complex collaborative tasks to be explored.

Future work will take state estimation and obstacle avoidance into consideration, and robust methods such as [19]–[21] will be exploited in the design of the distributed control protocol.

References

[1] J. Wang, A. Lanzon, and I. R. Petersen, "Robust output feedback consensus for networked negative-imaginary systems," *IEEE Transactions on Automatic Control*, vol. 60, no. 9, pp. 2547–2552, 2015.

[2] Z. Wu, Z. Guan, X. Wu, and T. Li, "Consensus based formation control and trajectory tracing of multi-agent robot systems," *Journal of Intelligent & Robotic Systems*, vol. 48, no. 3, pp. 397–410, 2007.

[3] H. Du, S. Li, and X. Lin, "Finite-time formation control of multiagent systems via dynamic output feedback," *International Journal of Robust and Nonlinear Control*, vol. 23, no. 14, pp. 1609–1628, 2013.

[4] J. A. Fax and R. M. Murray, "Information flow and cooperative control of vehicle formations," *IEEE Transactions on Automatic Control*, vol. 49, no. 9, pp. 1465–1476, 2004.

[5] M. Porfiri, D. G. Roberson, and D. J. Stilwell, "Tracking and formation control of multiple autonomous agents: A two-level consensus approach," *Automatica*, vol. 43, no. 8, pp. 1318–1328, 2007.

[6] M. Turpin, N. Michael, and V. Kumar, "Decentralized formation control with variable shapes for aerial robots," in *Proceeding of the IEEE International Conference on Robotics and Automation (ICRA)*, 2012, pp. 23–30.

[7] X. Dong, B. Yu, Z. Shi, and Y. Zhong, "Time-varying formation control for unmanned aerial vehicles: Theories and applications," *IEEE Transactions on Control Systems Technology*, vol. 23, no. 1, pp. 340–348, 2015.

[8] B. Crowther, A. Lanzon, M. Maya-Gonzalez, and D. Langkamp, "Kinematic analysis and control design for a nonplanar multirotor vehicle," *AIAA Journal of Guidance, Control, and Dynamics*, vol. 34, no. 4, pp. 1157–1171, 2011.

[9] A. Lanzon, A. Freddi, and S. Longhi, "Flight control of a quadrotor vehicle subsequent to a rotor failure," *AIAA Journal of Guidance, Control, and Dynamics*, vol. 37, no. 2, pp. 580–591, 2014.

[10] W. Ren and R. W. Beard, "Consensus seeking in multiagent systems under dynamically changing interaction topologies," *IEEE Transactions on Automatic Control*, vol. 50, no. 5, pp. 655–661, 2005.

[11] H. Zhang, F. L. Lewis, and Z. Qu, "Lyapunov, adaptive, and optimal design techniques for cooperative systems on directed communication graphs," *IEEE Transactions on Industrial Electronics*, vol. 59, no. 7, pp. 3026–3041, 2012.

[12] D. S. Bernstein, *Matrix mathematics: Theory, facts, and formulas with application to linear systems theory*. Princeton University Press Princeton, 2005, vol. 41.

[13] M. K. Mohamed and A. Lanzon, "Design and control of novel tri-rotor UAV," in *Proceedings of the 2012 UKACC International Conference on Control*, Cardiff, UK, 2012, pp. 304–309.

[14] J. Hu and A. Lanzon, "An innovative tri-rotor drone and associated distributed aerial drone swarm control," *Robotics and Autonomous Systems*, vol. 103, pp. 162–174, 2018.

[15] A. Isidori, *Nonlinear control systems*. Springer-Verlag, 1995.

[16] A. L. D. Franco, H. Bourlès, E. R. De Pieri, and H. Guillard, "Robust nonlinear control associating robust feedback linearization and H_∞ control," *IEEE Transactions on Automatic Control*, vol. 51, no. 7, pp. 1200–1207, 2006.

[17] Y. Lv, Z. Li, Z. Duan, and G. Feng, "Novel distributed robust adaptive consensus protocols for linear multi-agent systems with directed graphs and external disturbances," *International Journal of Control*, vol. 90, no. 2, pp. 137–147, 2017.

[18] X. Dong and G. Hu, "Time-varying formation control for general linear multi-agent systems with switching directed topologies," *Automatica*, vol. 73, pp. 47–55, 2016.

[19] J. Wang, A. Lanzon, and I. R. Petersen, "Robust cooperative control of multiple heterogeneous negative-imaginary systems," *Automatica*, vol. 61, pp. 64–72, 2015.

[20] A. Lanzon and H.-J. Chen, "Feedback stability of negative imaginary systems," *IEEE Transactions on Automatic Control*, vol. 62, no. 11, pp. 5620–5633, 2017.

[21] Z. Song, A. Lanzon, S. Patra, and I. R. Petersen, "Robust performance analysis for uncertain negative-imaginary systems," *International Journal of Robust and Nonlinear Control*, vol. 22, no. 3, pp. 262–281, 2012.